Journal of Psychiatric Research 115 (2019) 129–141

Contents lists available at ScienceDirect

Journal of Psychiatric Research

journal homepage: www.elsevier.com/locate/jpsychires

MicroRNA-140-5p: A novel circulating biomarker for early warning of late-onset post-stroke depression

Huai-bin Liang[a], Ji-rong He[b,1], Xuan-qiang Tu[a], Kai-qi Ding[a], Guo-Yuan Yang[a], Yu Zhang[c,**], Li-li Zeng[a,*]

[a] Department of Neurology, Ruijin Hospital, School of Medicine, Shanghai Jiao Tong University, Shanghai, 200025, China
[b] Department of Neurology, Ruijin Hospital Luwan Branch, School of Medicine, Shanghai Jiao Tong University, Shanghai, 200020, China
[c] Department of Neurology, Ruijin Hospital North, School of Medicine, Shanghai Jiao Tong University, Shanghai, 201801, China

ARTICLE INFO

Keywords:
Biomarker
Depression
Ischemia
microRNA
Stroke

ABSTRACT

We aimed to explore the circulating microRNAs biomarkers in the acute stage following cerebral ischemia to earlier warn late-onset post-stroke depression (PSD). A total of 251 consecutive patients with acute ischemic stroke were recruited. They were divided into three groups depending on whether PSD had occurred at 2 weeks or 3 months since stroke: early-onset PSD, late-onset PSD, and non-depressed group. Microarray assay was conducted to identify the different expression profiles of plasma miRNAs. Comprehensive bioinformatics analysis for their integrating putative target genes was performed. The key miRNA was validated in a larger cohort and its function was further studied in ischemic mice brain. We screened three differentially expressed miRNAs in the late-onset PSD individuals, miR-140-5p and miR-221-3p were significantly upregulated while miR-1246 was downregulated. The bioinformatics analysis demonstrated that their predicted target genes were mainly enriched in axon development and Ras signaling pathway. Logistic regression analysis revealed that miR-140-5p was an independent risk factor for late-onset PSD ($P = 0.017$, OR = 2.313, 95%CI 1.158 to 4.617). The miR-140-5p expression on admission was significantly positively correlated with HDRS scores assessed at 3 months after stroke ($P = 0.0007$). The predictive value of miR-140-5p for late-onset PSD is 83.3% sensitivity and 72.6% specificity (AUC = 0.8127, $P < 0.0001$). AAV-mediated overexpression of miR-140-5p decreased the protein level of IL1rap, IL1rapl1, VEGF, and MEGF10 in the ischemic mouse hippocampus and inhibited neurogenesis and capillary density. MiR-140-5p might be involved in the pathogenesis of late-onset PSD and used as a novel early warning biomarker.

1. Introduction

Post-stroke depression (PSD) is considered as one of the most frequent psychiatric complications of stroke (K Dar et al., 2017; Robinson and Jorge, 2016), About one-third of stroke survivors suffer from major depression either in the early or late stages after stroke (Hackett and Pickles, 2014). PSD is significantly associated with a worse functional outcome and higher mortality and is considered to be the worst prognostic factor for patients returning to work (Sturm et al., 2004). As a result, early recognition, prevention, and treatment for PSD are vital to the recovery and prognosis of stroke survivors.

According to the period between stroke event and the onset of PSD, PSD is divided into early-onset and late-onset. Early-onset PSD is defined as depression occurring in the acute stage two weeks following ischemia, while late-onset PSD occurs more than two weeks in the recovery or sequelae stage after a stroke (Wongwandee et al., 2012; Shi et al., 2015; Sun et al., 2014; Zhao et al., 2018). Compared with early-onset PSD, late-onset PSD had higher morbidity, worse prognosis and higher rates of misdiagnosis. Studies have shown that the prevalence of PSD varies with different time point, there exists a trend of rising firstly and then falling in the first year, and the highest incidence of depression just falls in the first few months following stroke (Bour et al., 2010, 2011). Notably, studies have revealed that if the onset is within few days since the stroke, then the possibility of spontaneous remission is

* Corresponding author. Department of Neurology, Ruijin Hospital, School of Medicine, Shanghai Jiao Tong University, China, 197 Ruijin Er Road, Shanghai, 200025, China.
** Corresponding author.
E-mail addresses: zyb1146@rjhn.com.cn (Y. Zhang), zll11131@rjh.com.cn (L.-l. Zeng).
[1] co-first author.

https://doi.org/10.1016/j.jpsychires.2019.05.018
Received 10 February 2019; Received in revised form 12 April 2019; Accepted 16 May 2019

likely high, however, the remission opportunities are minimal if the onset is more than seven weeks after a stroke (Andersen et al., 1994). According to a national survey in China, PSD at 3 months was highly predictive of disability at 5-year follow up (Yang et al., 2016). In addition, early-onset PSD occurs during hospitalization, doctors can early identify through clinical ward rounds and necessary neuropsychological tests. However, late-onset PSD patients couldn't be diagnosed timely because stroke survivors and their caregivers often neglect the abnormal mood changes after hospital discharge. Hence, how to early warn latent late-onset PSD patients is more challenging but rewarding.

In recent years, the emergence of small non-coding RNAs as a major gene expression regulator has attracted much attention in the pathophysiology of various diseases. Among them, microRNAs (miRNAs) are the most studied and most comprehensive (Wang et al., 2016). MiRNAs expression fingerprints can reflect literally the activation processes of specific pathological pathways. Remarkably, miRNAs are fairly stable in extracellular fluid (Larrea et al., 2016) and there exist some miRNAs highly expressed in the nervous system (Cao et al., 2016). Another significant advantage for central nervous system (CNS) diseases is that miRNAs are able to cross the blood-brain barrier (BBB), in the form of being delivered by naturally occurring exosomes (Narahari et al., 2017). Thence, circulating miRNAs hold great promise as a non-invasive and quantitative indicator for diagnosis and prognostic assessment in many diseases including PSD. In recent years, numerous studies have revealed that miRNAs are closely associated with stroke (miR-210, -124 and 140-5p etc.), major depressive disorder (MDD) (such as let-7b, -7c, miR-1202, -124-3p) and PSD (miR-137, -92a-3p, −211 and-300 etc.). There is growing evidence suggesting that circulating miRNAs could be used as potential biomarkers for the disease state, trait, or could act as mediators of response to treatment in depression. (Kim et al., 2019; Lopez et al., 2018; Tavakolizadeh et al., 2018). However, its relation with late-onset PSD remains unclear.

In the present study, we were interested in studying the epigenetic change in miRNA levels. Aiming to obtain plasma miRNA biomarkers for early warning of late-onset PSD, we compared the differences of plasma miRNAs expression profiles in the early-onset PSD, late-onset PSD, and non-depressed stroke patients. Then, a comprehensive enrichment analysis for their putative target genes was performed by bioinformatics tools to discern the underlying mechanism. The key miRNA was validated and evaluated for its potential as a warning marker of late-onset PSD in a large cohort of patients. We also conducted an in vivo functional study in cerebral ischemic mice to investigate the effect of key microRNA hyperexpression on hippocampal neurogenesis, pro-angiogenic and the protein levels of predicted targets.

2. Materials and methods

2.1. Study subjects

The present study has been approved by the Medical Ethics Committee of the Ruijin Hospital, Shanghai Jiao Tong University School of Medicine. All patients or their legally authorized representative (LAR) had signed informed consent forms. A total of 251 patients with acute ischemic stroke were consecutively recruited during May 2013 and September 2014, the data source is the same as previously reported (Zhang et al., 2017, 2016). Inclusion criteria: (1) clinical signs and symptoms was consistent with the diagnosis of an acute ischemic stroke and confirmed by CT or MRI at the time of admission; (2) Age > 18 years old; (3) within 7 days of the symptoms onset; (4) anticipated life expectancy of at least 6 months; (5) Subjects were willing and able to return for protocol requiring follow-up visits. Exclusion criteria: (1) History of major depressive disorder or other mental or emotional disorders; (2) Family history of depression; (3) Patients with disturbance of consciousness could not satisfy neuropsychological examination; (4) Patients with aphasia, hearing impairment, severe comprehension deficit or cognitive dysfunction that might preclude a verbal interview; (5) Any other serious illness that might threaten the patient's life or recovery from stroke. On the day of admission, all clinical data were recorded, including age, gender, education level, vascular risk factors (hypertension, diabetes, heart disease, and hyperlipidemia), as well as a history of stroke. Acute stroke-related neurological functional impairments was evaluated using the National Institutes of Health Stroke Scale (NIHSS), which incorporates assessment of language, motor function, sensory loss, consciousness, visual fields, extraocular movements, coordination, neglect, and speech (Harrison et al., 2013). The routine laboratory analysis including hemoglobin blood glucose (HbA1c), fasting blood glucose and several blood lipid indexes like total cholesterol (TC), triglyceride (TG), high-density lipoprotein cholesterol (HDL-C), low-density lipoprotein cholesterol (LDL-C), apolipoprotein A (Apo-A), apolipoprotein B (Apo-B) were performed immediately after hospitalization. Cranial CT or MRI scan was utilized to evaluate the lesion location and size, and infarct volume was calculated using the ABC/2 methods as reported (Sims et al., 2009). Cervical Doppler echography, CTA or MRA was conducted to assess the offending vessel and the stenosis level of intra- and extracranial artery. Peripheral blood samples from acute ischemic stroke patients were collected within 24 h after admission. Total 4-ml whole blood was collected into a vacutainer blood collection tube and then left at room temperature for 30 min to allow complete coagulation. Blood samples were then fractionated by centrifugation at 3,000 g for 15 min at 4 °C. The plasma layer was then aliquoted and stored at −80 °C for subsequent experiments. The other necessary examinations and treatment for stroke patients were corresponding to the Chinese guidelines for secondary prevention of ischemic stroke and transient ischemic attack (Wang et al., 2017).

2.2. Assessment of depression

The Diagnostic and Statistical Manual of Mental Disorders IV (DSM-IV) was used for the diagnosis of depressive disorders. Specifically, patients with a diagnosis of mood disorder due to stroke with depressive features must have depressed mood or loss of interest or pleasure along with at least two but less than five symptoms of major depression lasting 2 weeks or longer (Robinson and Jorge, 2016). Aside from the gold standard, the Hamilton Depression Rating Scale 17 items (HDRS, also abbreviated HAMD) was applied as a screening test and to quantify the severity of depressive symptoms. The assessment procedure of DSM-IV and HDRS was carried out by bridle-wise clinicians at two different time points: 2–3 weeks and 3 months after stroke. During the follow-up, if the stroke patient was found to have depression, antidepressant medication will be given immediately. According to whether were depressed within the first 2–3 weeks, all patients were divided into early-onset PSD group or non-early-onset PSD group. After a three-month follow-up, the non-early-onset PSD patients was further separated into late-onset PSD groups and the control group (Fig. 1.). Subsequently, the study was conducted in two phases. During screening stage, under the premise of controlling for confounding variables by the matching factors, we selected 9 individuals from 3 groups (three cases each group) (Supplementary Table 1) used as microarray screening. In the validation stage, the candidate microRNA identified in the first phase was validated in a larger cohort.

2.3. MiRNA microarray

Human miRNA microarray (version 19, Agilent Technologies) was used to detect miRNAs profiles in the plasma of stroke patients. In brief, Total RNA was isolated using mirVana RNA isolation kit (Invitrogen, USA) and RNA quality was determined by using Bioanalyzer (Agilent, Santa Clara CA), RNA integrity number (RIN) score was required to > 7.0. Subsequently, the microarray experiment was performed by OE Biotech (Shanghai, China). Then oligonucleotide probes signals

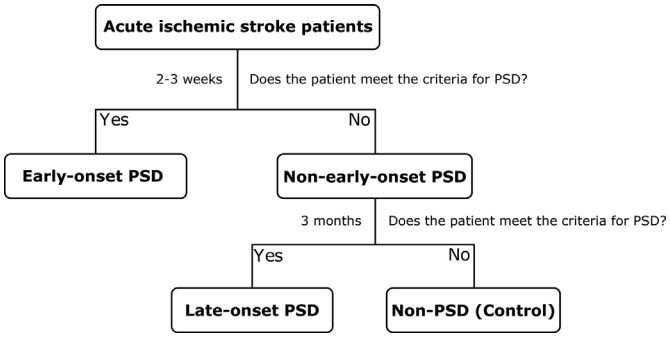

Fig. 1. Flow chart of the selection of the study group. The DSM-IV was used for the diagnosis criteria, the HDRS-17 was applied as a screening test and to quantify the severity of depressive symptoms. Abbreviations: DSM-IV, The Diagnostic and Statistical Manual of Mental Disorders IV; HDRS-17, Hamilton Depression Rating Scale 17 items, also abbreviated HAMD.

were extracted by Agilent Feature Extraction image analysis algorithm (AFE) and used for subsequent analysis.

2.4. Microarray data normalization and analysis

The analysis was performed under the R programming environment (R software version 3.5.0, http://www.r-project.org/) (Ihaka and Gentleman, 1996). Several Bioconductor R packages were used to achieve statistical computing and graphics rendering (López-Romero, 2011; Ritchie et al., 2015; Yu, 2018). Firstly, the data quality was evaluated and normalization was conducted, then the filter function was used to remove inferior quality probes based on the flag assigned by scan software. Limma package was utilized to conduct the differential expression analysis. To enhance reliability and reproducibility, we used two different background correction algorithms (AFE and RMA algorithm, respectively) (Chang et al., n.d.). The significance threshold was set at 0.05.

2.5. Target prediction and network analysis

The predicted targets of candidate miRNAs were generated by miRWalk 3.0 (Dweep et al., 2011), with setting the threshold p-value > 0.90. Gene Ontology (GO) functional enrichment analysis and Kyoto Encyclopedia of Genes and Genomes (KEGG) pathway enrichment analysis were performed by using clusterProfiler (Yu et al., 2012), p-value < 0.01 and q value < 0.05 were considered to be significantly enriched. A circos was depicted to display the interaction network relationship between the top-10 significantly enriched GO terms and candidate miRNAs (Krzywinski et al., 2009). For the target genes set of miR-140-5p, BioCarta pathway database and Jensen tissue database were also used for pathway and tissue enrichment analysis in Enrichr web server (Kuleshov et al., 2016).

2.6. Quantitative real-time RT-PCR validation

The validation cohort was generated as follows. During the 3-month follow-up, a total of 19 patients was excluded ultimately from the cohort (1 subject died, 2 subjects stroke relapsed, 1 experienced a severe systemic disease and 15 patients lost the follow-up). Along with the three-month follow-up was terminated, a total of 19 late-onset PSD patients and 168 controls were generated. Combining with the 43 early-onset PSD individuals, a total of 62 stroke survivors suffered PSD. Control subjects were chosen based 1:1 matched on age, gender, stroke location, stroke risk factors. Then the selected 62 control individuals and 62 PSD patients (including 19 late-onset and 43 early-onset) were brought into the validation dataset. Probe-based RT-PCR was used to validate the microarray results. The expression of each miRNAs was calculated by subtracting the Ct value of the control miRNA, cel-miR-39-3p.

2.7. Generation and in vivo injection of AAV vector

The virus AAV2/9-CMV-amiR-eGFP was chosen for transfecting the hippocampus (AAV-miR1405p group). A similar construct (AAV2/9-CMV-eGFP) without miR-140-5p and sterile PBS was used as controls (AAV-Ctrl group and PBS group). All virus vectors were purchased from OBio Technology (Shanghai, China), stored at $-80\,^{\circ}C$ until use. Adult male C57BL/6 mice weighing 20 g–25 g were anesthetized with xylazine (10 mg/kg, Sigma, San Louis, MO) and ketamine (100 mg/kg) intraperitoneally. AAV suspension with a titer of 2×10^{13} vg/mL was injected into the left dentate gyrus (DG) region (1.5 μl at 0.15 μl/min) using stereotaxic injection (coordinates, bregma: AP = −2.0, ML = −1.0, DV = −2.0). After vector delivery, the needle was left at the position for 5 min, then slowly withdrawn over 5 min. Then, mice were removed from the stereotactic apparatus and the incisions were closed with 4.0 silk suture. After sufficient awakening from anesthesia, animals were returned to their cages for long-term recovery. The methodological details of the cerebral ischemia model and the molecular assays such as qRT-PCR, WB, and immunofluorescence are shown in the **Supplementary Methods. 1**.

2.8. Statistical analysis

All data are expressed as the mean ± SD or median [25%,75%] and were analyzed using GraphPad Prism 6 (GraphPad Software, Inc., San Diego, CA). We first performed the normality test on each dataset using the Shapiro-Wilk test. Parametric tests were used if the dataset passes the normality test. Otherwise, non-parametric tests were used. Difference between groups was analyzed with One-way ANOVA, Student's t-test or Mann–Whitney test. Logistic regression was accomplished by SPSS software (SPSS Inc., Chicago, USA) and receiver operating characteristic (ROC) curves were utilized to figure out the cutoff value via GraphPad Prism 6. The p-value < 0.05 was regarded as statistically significant.

3. Results

3.1. Patient characteristics

There were no significant gender or age et al. biases between the groups in the screening cohort (Supplementary Table. 1). The demographic and clinical characteristics of the subjects in the validation cohort were summarized in Table 1. There were no significant differences in the distribution of age, sex, education level, cardiac disease, previous stroke, stroke etiology, lesion laterality and location, hyperlipidemia status, and blood lipid tests among three groups (all $P > 0.05$). Diabetes prevalence, fasting blood glucose and HbA1c were higher in late-onset PSD subjects than the remaining two groups (all $P < 0.05$). Besides that, the incidences of hypertension and carotid artery stenosis were much higher in early-onset subjects (all $P < 0.05$) in comparison with non-early-onset groups (Table 1).

3.2. MicroRNA expression profiles

The raw data composed of 62344 miRNA probes signals which represented 2027 human miRNAs was loaded into AgiMicroRna. The medians, as shown in Fig. 2A, located at the almost identical level after performing data normalization, which indicated a perfect effect. Afterward, AFE and RMA methods generated not exactly the same output tables. Having noted these issues, the common miRNAs were regarded as the most promising and stable ones. Fig. 2B shows the volcano plot of expression distribution feature of all miRNAs calculated by the RMA algorithm. The heatmap in Fig. 2C demonstrates the

Table 1
Clinical parameters of control subjects and PSD patients in the validation cohort.

	Control	Early-onset PSD	Late-onset PSD	P value
	N = 62	N = 43	N = 19	
Age	65.56 ± 11.95	68.02 ± 9.86	66.89 ± 7.36	0.507
Females, n (%)	21 (33.9)	17 (39.5)	5 (26.3)	0.591
Education, (High school or above)	34 (54.8)	23 (53.5)	11 (57.9)	0.950
Hypertension, n (%) [a]	40 (64.5)	37 (86.0)	14 (73.7)	0.049
Hyperlipidemia, n (%)	28 (45.2)	20 (46.5)	8 (42.1)	0.950
Diabetes, n (%) [b]	15 (24.2)	15 (34.9)	10 (52.6)	0.061
Cardiac disease, n (%)	10 (16.1)	7 (16.3)	1 (5.3)	0.386
Previous stroke, n (%)	9 (14.5)	10 (23.3)	3 (15.8)	0.509
Total number of strokes, mean ± SD	1.16 ± 0.41	1.30 ± 0.60	1.26 ± 0.73	0.400
Carotid Artery Stenosis, n (%) [a]	28 (50.0)	31 (77.5)	8 (47.1)	0.014
NHISS score on admission [b]	2.74 ± 2.04	4.86 ± 3.19	4.21 ± 2.35	< 0.001
NHISS score > 3 on admission, n (%) [b]	18 (29.0)	29 (67.4)	10 (52.6)	< 0.001
Stroke Etiology (TOAST)				0.687
Large-artery atherosclerosis	27 (43.5)	20 (46.5)	10 (52.6)	
Cardioembolism, n (%)	3 (4.8)	0 (0.0)	1 (5.3)	
Small vessel disease, n (%)	21 (33.9)	14 (32.6)	5 (26.3)	
Other, n (%)	0 (0.0)	0 (0.0)	0 (0.0)	
Unknown, n (%)	11 (17.7)	9 (20.9)	3 (15.8)	
Stroke laterality				0.377
Left, n (%)	35 (56.5)	18 (41.9)	10 (52.6)	
Right, n (%)	26 (41.9)	20 (46.5)	9 (47.4)	
Both, n (%)	1 (1.6)	5 (13.6)	0 (0.0)	
Stroke location				0.407
Frontal lobe, n (%)	4 (6.5)	2 (4.7)	0 (0.0)	
Parietal lobe, n (%)	3 (4.8)	0 (0.0)	0 (0.0)	
Occipital lobe, n (%)	0 (0.0)	0 (0.0)	0 (0.0)	
Thalamus, n (%)	4 (6.5)	1 (2.3)	0 (0.0)	
Brainstem, n (%)	13 (21.0)	8 (18.6)	5 (26.3)	
Basal ganglia or lateral ventricles, n (%)	30 (48.4)	20 (46.5)	9 (47.4)	
Cerebellum, n (%)	1 (1.6)	0 (0.0)	2 (10.5)	
Multiple locations, n (%)	6 (9.7)	12 (27.9)	3 (15.8)	
Distance of lesion from frontal pole (cm)	6.04 ± 2.12	5.58 ± 2.12	6.57 ± 1.64	0.350
Infarct volume (ml),	0.46 [0.16,6.34]	0.66 [0.22,3.15]	0.50 [0.22,2.39]	0.504
HDRS: 2–3 weeks [a,c]	2 [1,4]	9 [8,15]	4 [3,4]	< 0.001
HDRS: 3 months [a,b]	1 [0.5,3]	8 [7,11]	9 [9,10]	< 0.001
Fasting blood-glucose, (mmol/L) [b]	6.19 ± 2.51	5.83 ± 1.83	7.10 ± 2.33	0.008
HbA1c, (%) [b]	6.35 ± 1.55	6.43 ± 1.22	8.17 ± 2.26	< 0.001
TG, (mmol/L)	1.83 ± 0.85	1.79 ± 0.81	1.74 ± 0.92	0.917
TC, (mmol/L)	4.75 ± 1.12	4.60 ± 1.32	4.61 ± 1.08	0.798
HDL-C, (mmol/L)	1.08 ± 0.28	1.08 ± 0.28	1.12 ± 0.30	0.851
LDL-C, (mmol/L)	3.00 ± 0.94	2.88 ± 1.12	2.82 ± 1.01	0.742
ApoA, (g/L)	1.18 ± 0.22	1.17 ± 0.25	1.16 ± 0.21	0.934
ApoB, (g/L)	1.01 ± 0.28	0.99 ± 0.33	1.00 ± 0.26	0.935

Notes: Data are mean ± SD, median [25%,75%] or number of patients (percentage of total). Differences between groups were analyzed with One-way ANOVA. Post-hoc tests were run to confirm where the differences occurred between the pairwise comparisons, [a] Represents control versus early-onset PSD, [b]Represents control versus late-onset PSD, [c]Logistic regression analysis to identify independent clinical predictors for late-onset PSD patients.
Abbreviations: HDRS, Hamilton Depression Rating Scale; HbA1C, glycosylated hemoglobin; TG, triglyceride; TC, total cholesterol; HDL-C, high density lipoprotein cholesterol; LDL-C, low density lipoprotein cholesterol; ApoA, apolipoprotein A; ApoB, apolipoprotein B.

differential expression miRNAs based RMA-algorithm, separately. Venn diagram was used to show how many miRNAs were common and exclusively expressed. Only 3 miRNAs were obtained ultimately (miR-140-5p, miR-221-3p, miR-1246). Fig. 2D presents the detailed information.

Three differentially expressed miRNAs were ultimately identified. MiR-140-5p (P = 0.0016, log2 (fold change) = 3.5) (fold change, FC), and miR-221-3p (P = 0.0479, log2(FC) = 7.48) had significantly higher expression in late-onset PSD group than early-onset PSD and controls, meanwhile, miR-1246 (P = 0.0238, log2(FC) = −1.8) had lower expression than other individuals. RMA's method generated a similar result as above. The distribution feature of candidate miRNAs was shown in Fig. 2E.

3.3. Functional and pathway enrichment analysis

According to miRwalk website, a total of 6979 target genes for the candidate miRNAs were generated. The top 30 enriched GO BP terms are exhibited in Fig. 3A, and the top 30 clustered KEGG pathway term are displayed in Fig. 3B. Axon development and Ras protein signal transduction were the most significantly enriched GO biological processes. As for KEGG, the targets are significantly enriched in the Ras signaling pathway, FoxO signaling pathway, MAPK signaling pathway, and axon guidance. In addition, a circos plot was constructed to display the miRNA-target gene-pathway crosslinking network, which makes it easier to understand the dominant biological regulation function of each miRNA (Fig. 3C).

3.4. Functional annotation and validation of candidate miRNA-140-5p

In terms of miR-140-5p, a large amount of neurological system related biological process were enriched, including axonogenesis, neuron projection morphogenesis, forebrain development, and Ras protein signal transduction. According to the TISSUES 2.0 transcriptomic expression datasets (http://tissues.jensenlab.org/), the targets of miR-140-5p were predominantly enriched in CNS such as the brain,

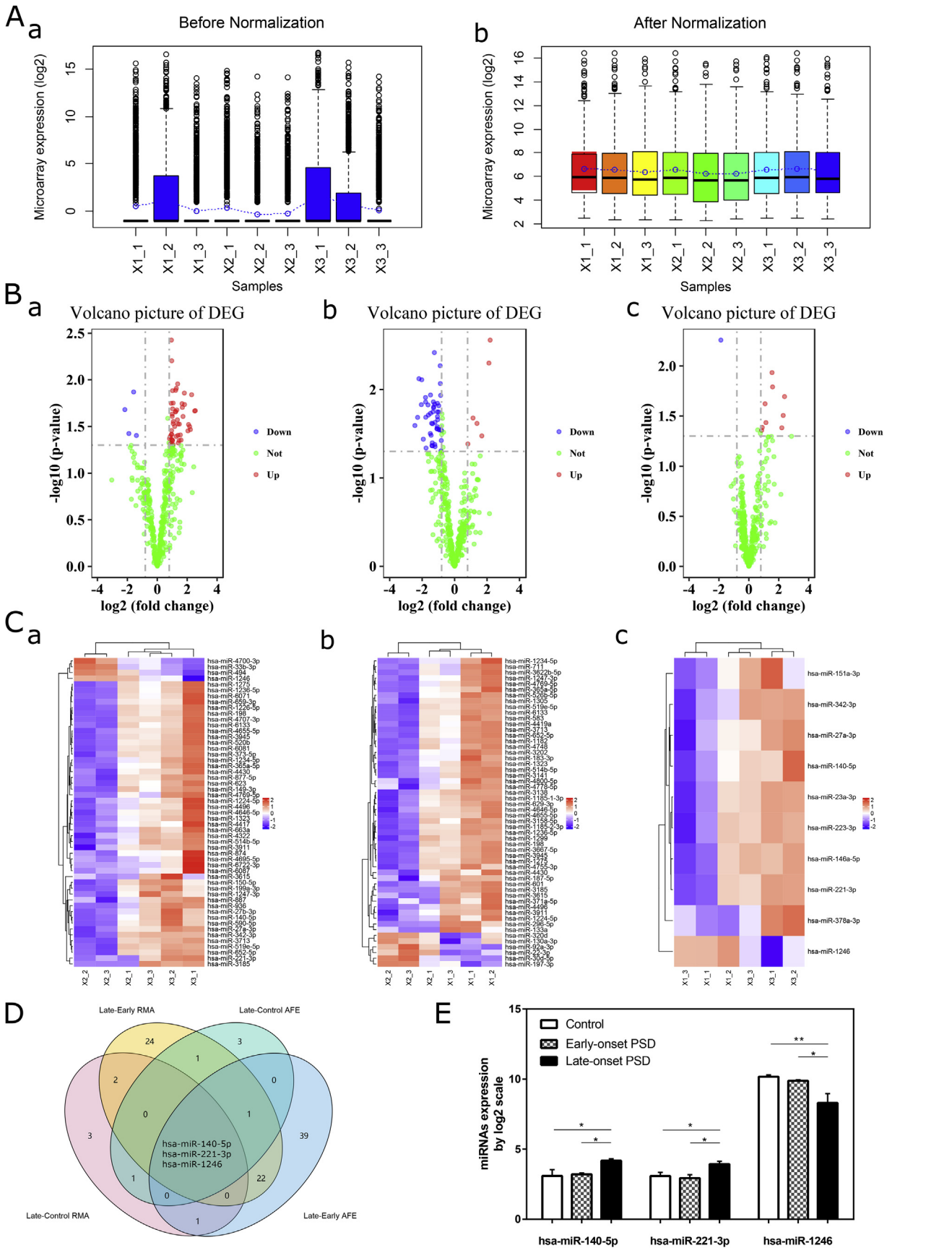

(caption on next page)

Fig. 2. Microarray analysis of circulating miRNA profiles in patients with early-onset PSD, late-onset PSD, and controls. **A.** Box plots of results of data normalization. (a) Raw data before normalization; (b) After RMA normalization, all nine intensity distributions appear consistent. Notes: Each blue box represents a sample before normalization, then each box of different color represents a sample. The x coordinate represents the samples and the y-coordinate represents the microRNA expression values in log2 scale. The midline of the box plot represents the microRNA expression median and the whiskers represent the interquartile range. **B**. Volcano plot showing the distribution of the miRNAs expression fold changes and their negative log10-transformed p-value. MicroRNAs fulfilling the criteria (P-value < 0.05 and fold change > 1.5) were regarded as DEMs. MiRNAs expression distribution between late-onset and early-onset PSD, (a); early-onset PSD and controls, (b); late-onset PSD and controls, (c). Notes: DEMs that were upregulated depicted as red dots, downregulated as blue, while those with no significance are shown in gray. **C.** Heatmap of differentially expressed miRNAs. (a) Unsupervised hierarchical clustering of DEMs between late-onset PSD and early-onset PSD. (b) DEMs between early-onset PSD and controls. (c) DEMs between late-onset PSD and controls. Notes: Each row corresponds to one miRNA, and each column corresponds to one sample. The unregulated miRNAs are depicted in red color whereas the down-regulated miRNAs are depicted in blue color. **D.** Venn diagram showing the comparison of two different methods for differential expression miRNAs analysis results between late-onset and non-late-onset PSD (early-onset PSD and controls, respectively), which identified only three miRNAs commonly appearing in four datasets. Notes: Early-Late AFE represent the results between early-onset and late-onset PSD using AFE algorithm. So on and so forth. **E.** The barplot shows the most significant changed miRNAs for late-onset PSD, including hsa-miR-140-5p, hsa-miR-221-3p and hsa-miR-1246. * represents $P < 0.05$; ** represents $P < 0.01$. Abbreviations: DEMs, differentially expressed miRNAs. (For interpretation of the references to color in this figure legend, the reader is referred to the Web version of this article.)

hypothalamus, occipital lobe and temporal lobe (Fig. 4A). We took full advantage of the well-known BioCarta pathways, the targets of miR-140-5p were mainly functionally annotated in CREB signal, G-protein coupled receptor pathway, IGF-1 and PDGF signal (Fig. 4B), implying that transmembrane receptor protein tyrosine kinase family accounts for a significant advantage.

In particular, miR-140-5p was the top differential miRNA between the late-onset PSD and non-late-onset PSD groups and was expressed at remarkably higher levels in late-onset PSD ($P = 0.0016$, log2(FC) = 3.5, by AFE; $P = 0.0041$, log2(FC) = 1.03, by RMA). MiR-140-5p were further verified with qRT-PCR in a validation cohort. Consistent with the array results, miR-140-5p was indeed significantly elevated in late-onset patients as compared with counterparts in the validation cohort (Fig. 4C) ($P < 0.0001$, separately).

3.5. Identification of miR-140-5p as potential biomarker of late-onset PSD

Logistic regression analysis demonstrated that only miR-140-5p and HbA1c were the independent risk factors for late-onset PSD occurrence ($P = 0.019$, OR = 2.283, 95CI% 1.145 to 4.549; $P = 0.044$, OR = 1.410, 95%CI 1.010 to 1.970. respectively). After adjustment for other confounding factors including the variables diabetes, fasting blood-glucose, NIHSS, NIHSS > 3 and multiple locations. the contribution of miR-140-5p was still significant ($P = 0.017$, OR = 2.313). The p-value of HbA1c slightly decreased ($P = 0.054$, OR = 1.392) (Table 2). The AUC for miR-140-5p is 0.8127 ($P < 0.0001$, 95%CI 0.715 to 0.910) with 83% sensitivity and 72% specificity (Fig. 4D), with a cutoff value $\Delta Ct = -10.2$. Remarkably, the miR-140-5p expression level on admission was significantly positively correlated with the HAMD scores assessed at 3 months among non-early-onset PSD patients ($P = 0.0007$, $r = 0.4625$) (Fig. 4E), while this relationship did not exist in early-onset PSD patients.

3.6. AAV vector-mediated miR-140-5p overexpression in the hippocampus of cerebral ischemic mouse

To determine the transfer efficiency of AAV vector in the brain of cerebral ischemic mouse. eGFP expression was assessed at 28-day post-ischemic operation via fluorescent microscope. The green fluorescence marker was observed in the left hippocampal DG and CA3 region after gene transfer. Real-time PCR assay confirmed that miR-140-5p was highly upregulated in the left hippocampus in AAV-miR1405p-treated mice compared with the AAV-Ctrl-treated and PBS-treated mice ($p < 0.0001$), indicating that miR-140-5p could be overexpressed effectively through gene transfer in the hippocampus of the cerebral ischemic mouse (Fig. 5A).

3.7. MiR-140-5p overexpression inhibited neurogenesis and capillary proliferation in the hippocampus

To determine whether miR-140-5p overexpression influenced neurogenesis, neural precursor cells were measured by immunofluorescence staining. The DCX reactive area was significantly reduced in the DG of AAV-miR1405p-treated mice compared with the AAV-Ctrl treated and PBS-treated mice ($P < 0.001$ and $P < 0.0001$. respectively). Lower DCX positive cells numbers were also observed in AAV-miR1405p-treated mice (both $P < 0.0001$). This results indicating that miR-140-5p have an effect of neurogenesis suppression and could inhibit new hippocampal cells generated in the DG (Fig. 5B).

Microvessel density was also examined to determine whether the overexpression of miR-140-5p would influence the capillary density in the DG region. CD31 staining demonstrated that the microvessel density pixels were greatly decreased in the AAV-miR1405p-treated mice in the DG compared with AAV-Ctrl treated and PBS-treated mice ($P < 0.001$ and $P < 0.0001$. respectively), suggesting that miR-140-5p have inhibition effect on focal capillary proliferation of hippocampus (Fig. 5C).

3.8. MiR-140-5p overexpression decreased neuroplasticity and angiogenesis-related protein expression

Considering that the prediction of the microRNA targets was generated by miRNA target prediction algorithms based on the binding sites in the 3′UTRs of the mRNAs, it is necessary to investigate test whether some of the predicted target genes were downregulated indeed by miR-140-5p overexpression. Most commonly, miRNA induce target mRNA degradation or impede target protein translation (in that case, mRNA levels may be unchanged) (Catalanotto et al., 2016; Ruike et al., 2008). We directly detected some promising and representative protein expression using Western blotting, such as angiogenesis-related Vegfa, neuroplasticity-related IL1rap and IL1rapl1, phagocytosis and apoptosis-related protein like Bcl-2, Megf10, neuronal development and growth related Egfr. AAV-miR1405p-treated had no change in Megf10 and Egfr protein expression compared with controls. However, miR-140-5p overexpression exhibited a significant decrease in Vegfa (both $P < 0.05$), Bcl-2 (both $P < 0.001$), IL1rap (both $P < 0.05$) and IL1-rapl1 (both $P < 0.05$) protein levels compared with the AAV-Ctrl and PBS-treated group (Fig. 6).

4. Discussion

At present, the pathogenesis of PSD remains unclear. The biological determinism and psychosocial vulnerability were the two main hypotheses (Santos et al., 2009). Studies have shown that the evolution and mechanism of late-onset PSD were different from early-onset PSD. Compared with late-onset, early-onset PSD usually has a shorter course and may be more prone to spontaneous remission. Early-onset PSD

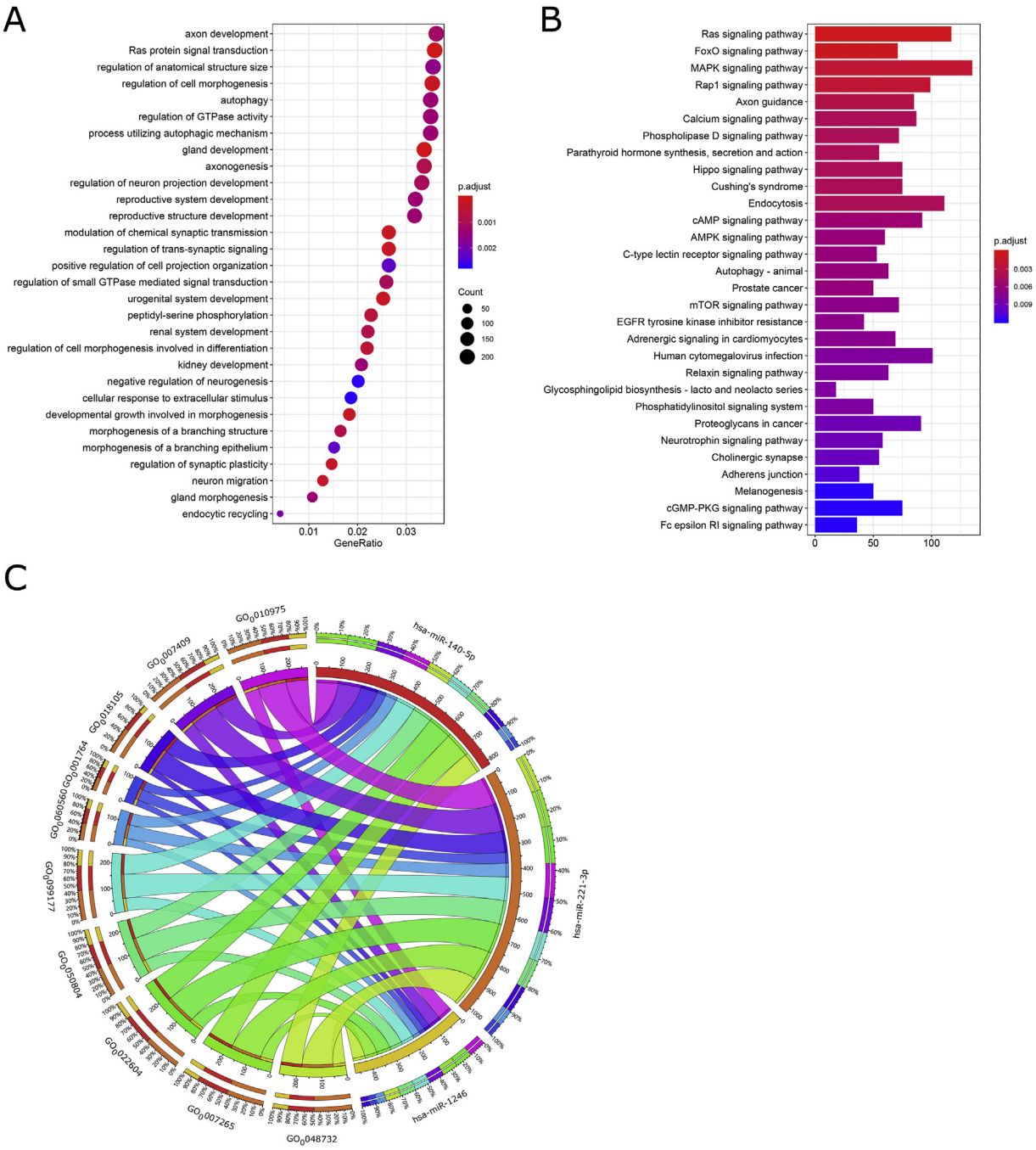

Fig. 3. Significantly enriched functional terms based on target genes of the three candidate miRNAs. **A.** Dot plot of significant GO Biological Process terms. **B.** Barplot of significant KEGG signaling pathways. **C.** A circos plot shows the connections of top 10 significantly enriched biological processes terms based on predicted target genes with their corresponding miRNAs. Here simplified method was utilized to remove redundant or highly similar GO terms. Notes: In plot A and B, top 25 (most significant) categories of each cluster was plotted. In plot C, GO_0048732: gland development; GO_0007265: Ras protein signal transduction; GO_0022604: regulation of cell morphogenesis; GO_0050804: modulation of chemical synaptic transmission; GO_0099177: regulation of trans-synaptic signaling; GO_0060560: developmental growth involved in morphogenesis; GO_0001764: neuron migration; GO_0018105: peptidyl-serine phosphorylation; GO_0007409: axonogenesis; GO_0010975: regulation of neuron projection development. BH-corrected P < 0.01 and q-value < 0.05 was considered statistically significant. Abbreviations: GO, Gene ontology; KEGG, Kyoto Encyclopedia of Genes and Genomes, BH, Benjamin-Hochberg.

represents a transient but immediate response to stroke based on the biochemical mechanisms (lesions of circuits responsible for mood control, changes in receptor regulation, the rate of neurotransmitter or enzyme synthesis etc.). Late-onset PSD may integrate more psychosocial factors, with delayed but lasting effects on mood (Berg et al., 2003). In the current study, we observed the different miRNAs expression between early-onset and late-onset depression after stroke, which suggested a distinct pathological mechanism might involve in the depressive episodes at different onset time. In line with the functional annotation of the differentially-expressed miRNAs' targets, axon development and Ras protein signal transduction are the most prominent biological process. This finding provided us with novel hints on the pathogenesis of late-onset PSD. Axon growth, also known as axonal growth, equivalent to some more specific terms used such as regeneration, sprouting, and plasticity. Alternatively, Ras-Raf-MAP kinase signaling cascades downstream of neurotrophic receptors is the key

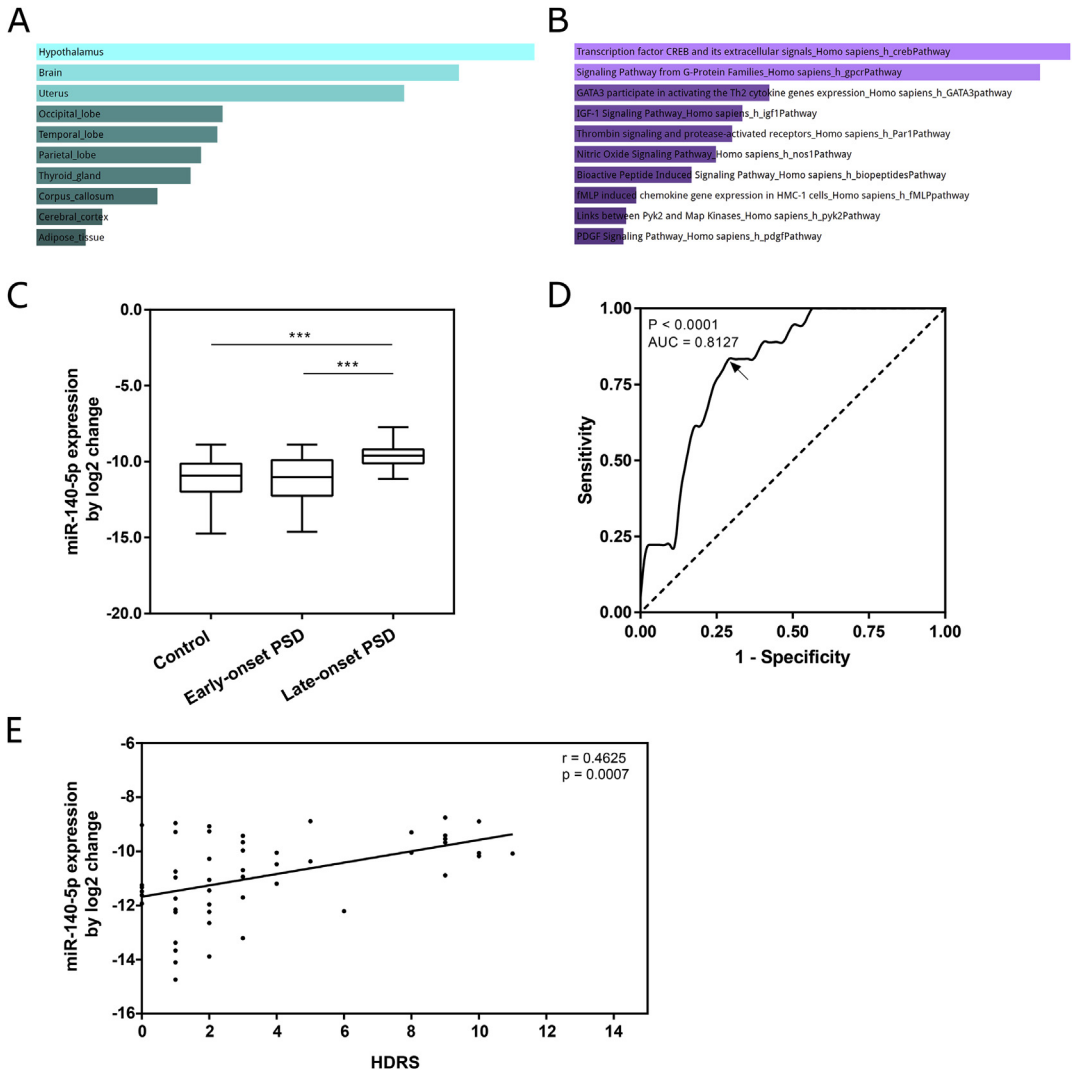

Fig. 4. Comprehensive enrichment analysis of predicted targets of miR-140-5p and the identification as a potential biomarker of late-onset PSD. **A.** Target genes corresponding to hsa-miR-140-5p are significantly enriched in the central nervous system (CNS) based on Enrichr web server and Jensen Tissue expression database. Sorted by p-value ranking. **B.** Significant enriched BioCarta pathway terms of hsa-miR-140-5p targets base on Enrichr web server. Sorted by a combined score. **C.** qRT-PCR analysis results of miR-140-5p in a validation cohort consists of early-onset, late-onset PSD and control groups. Data were mean ± SD; the P values were calculated by one-way ANOVA test. **D.** Receiver operating characteristic (ROC) curves for miR-140-5p as a potential biomarker to differentiate late-onset PSD individuals. **E.** Correlation between circulating miR-140-5p expression level on admission after acute ischemic stroke and HAMD score of non-early-onset PSD patients in three months. Notes: The normalized expression value of miR-140-5p is shown as ΔCt value. *** represents $P < 0.001$. Abbreviations: AUC, the area under the curve.

cell-signaling pathway that controls axon outgrowth (Goldberg, 2003). Therefore, in essence, these two biological processes are highly correlated. In adult mammalian CNS, axonal growth is deemed a form of spontaneous plasticity and is critical during the development of the nervous system and functional recovery after CNS injury. Not surprisingly in psychiatry, the neuroplasticity hypothesis is emerging as a novel but promising theory for the etiology of MDD. Scholars have realized that neuroplasticity, the remodeling process of brain structure and function, occurs throughout life, and positive neuroplasticity can be interrupted by psychosocial and biological factors during the rehabilitation stage of stroke patients. The axon growth related biological themes cluster results suggest that neural plasticity might be highly involved in the pathogenesis of late-onset PSD.

After harvesting three candidates miRNAs (miR-140-5p, -221-3p and −1246), we compared various tissues miRNAs expression data from the Human miRNA Tissue Atlas (Ludwig et al., 2016). Among

Table 2
Logistic regression analysis to identify independent clinical predictors for late-onset PSD patients.

Variable	B value	S.E. value	Wald value	P value	OR	CI (95%)
hsa-miR-140-5p	0.838	0.353	5.649	0.017	2.313	1.158–4.617
HbA1c	0.331	0.172	3.698	0.054	1.392	0.994–1.950
Constant	4.956	4.149	1.427	0.232	142.053	

Notes: Adjusted for diabetes, fasting blood-glucose, NIHSS scores.
Abbreviations: OR, odds ratio; CI, confidence interval; HbA1c, glycosylated hemoglobin.

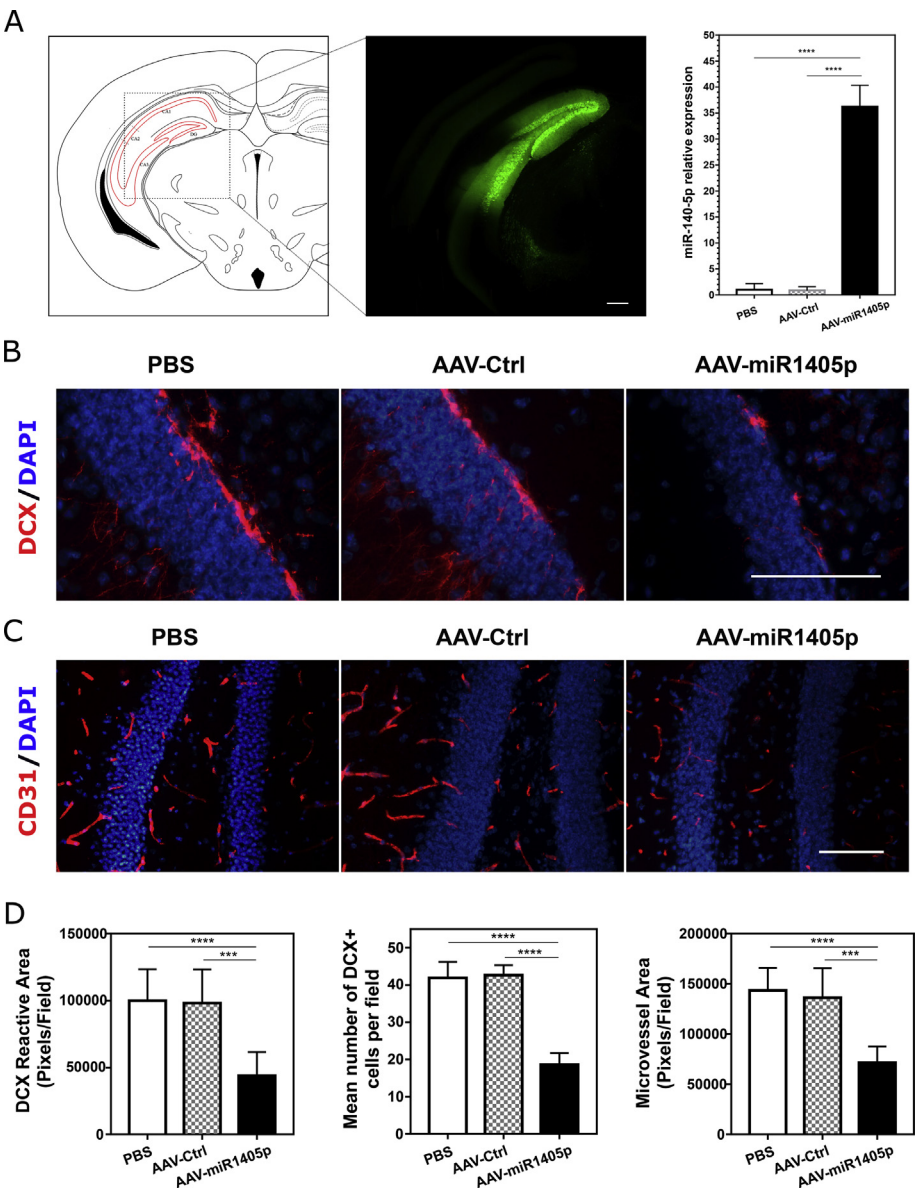

Fig. 5. Neurogenesis and capillary density were reduced in the DG region of AAV-miR1405p-treated mice. **A.** (a) Graphic illustration of a mouse brain coronal section and the region of interest box shows green fluorescence after AAV gene transfection. (b) Photomicrographs of stitching show the full view of the intense boundary of eGFP signal (green) around the DG region at 42 days after stereotactic injection (28 days post ischemic operation). Bar = 500 μm. (c) The bar graph shows the quantitative PCR analysis of miR-140-5p expression of the hippocampus area after AAV-miR1405p, AAV-Ctrl or PBS administration. Data are presented as mean ± s.d. ****P < 0.0001. **B.** (a) Representative photograph of CD31 immunostaining in the DG area of AAV-miR1405p, AAV-Ctrl or PBS-treated mice. Bar = 50 μm. (b) The bar graph shows the quantification of microvessel density per field from CD31 immunostaining brain sections. n = 5 per group. ***P < 0.001; ****P < 0.0001. **C.** (a) Representative photograph of doublecortin (DCX) immunostaining in the DG area of AAV-miR1405p, AAV-Ctrl or PBS-treated mice. Bar = 50 μm. (b) The bar graph shows the quantification of the DCX reactive area (up) and numbers of DCX positive cells (down) per field from DCX immunostaining brain sections. n = 5 per group. ***P < 0.001, ****P < 0.0001. (For interpretation of the references to color in this figure legend, the reader is referred to the Web version of this article.)

them, miR-140-5p is a tissue specificity miRNA (tissue specificity index > 0.85 among 61 tissue biopsies) and predominantly expresses in certain specific tissues or organs like brain, bone, and muscle. In addition, there is also literature confirming this fact that miR-140-5p is certainly brain-specific (Lin et al., 2011). Apart from the factors above, miR-140-5p also ranked at the first among differentially expressed miRNAs sorted by p-value, meaning there is a minimum chance that we make the wrong decision (false positives). So in the verification phase, we have chosen miR-140-5p to verify the reliability by qRT-PCR assay in a large cohort. And we confirmed the close relationship between miR-140-5p and late-onset PSD. Previous studies have already revealed that miR-140-5p played a vital but complicated role in certain neurological diseases including stroke, Parkinson's disease, Alzheimer's disease, epilepsy, multiple sclerosis, and autism spectrum disorder. Notably, the relationship with MDD or PSD has not been reported yet. To our knowledge, we firstly reported the correlation between miR-140-5p and late-onset PSD. In addition, we also found miR-140-5p was positively related with the severity of late-onset PSD. Acute ischemic stroke patients with a higher miR-140-5p on admission had more severe depressive symptoms three months after stroke. MiR-140-5p might be a novel biomarker to early predict late-onset PSD.

Currently, few studies about the blood biomarker in late-onset PSD had been reported. Li et al. demonstrated that lower serum BDNF level at admission could predict PSD occurring within 3 months with 73.2% sensitivity and 70.7% specificity (Li et al., 2014). Compared with BDNF, circulating miR-140-5p had higher predictive accuracy with 83.3% sensitivity and 72.6% specificity for late-onset PSD. In addition, our previous study showed that stroke patients with diabetes were more likely to develop late-onset PSD, and a raised glucose or HbA1c should alert one to future suffer from depression, especially late-onset PSD. The prediction efficiency of HbAlc was 61.1% sensitivity and 76.7% specificity (Zhang et al., 2017). In the present study, after adjusting for HbA1c, the multivariate logistic regression analysis showed that the association between miR-140-5p and late-onset PSD was still significant. Moreover, the discriminatory power of miR-140-5p was stronger than HbA1c.

Based on the above findings, we observed that the existence of the relationship between miR-140-5p and late-onset PSD, but the specific underlying mechanism remains unclear, so we conducted an in vivo study in cerebral ischemic mice to determine what miR-140-5p affected. It has been suggested that the dysfunction of hippocampus might be responsible for the MDD developing (Snyder et al., 2011).

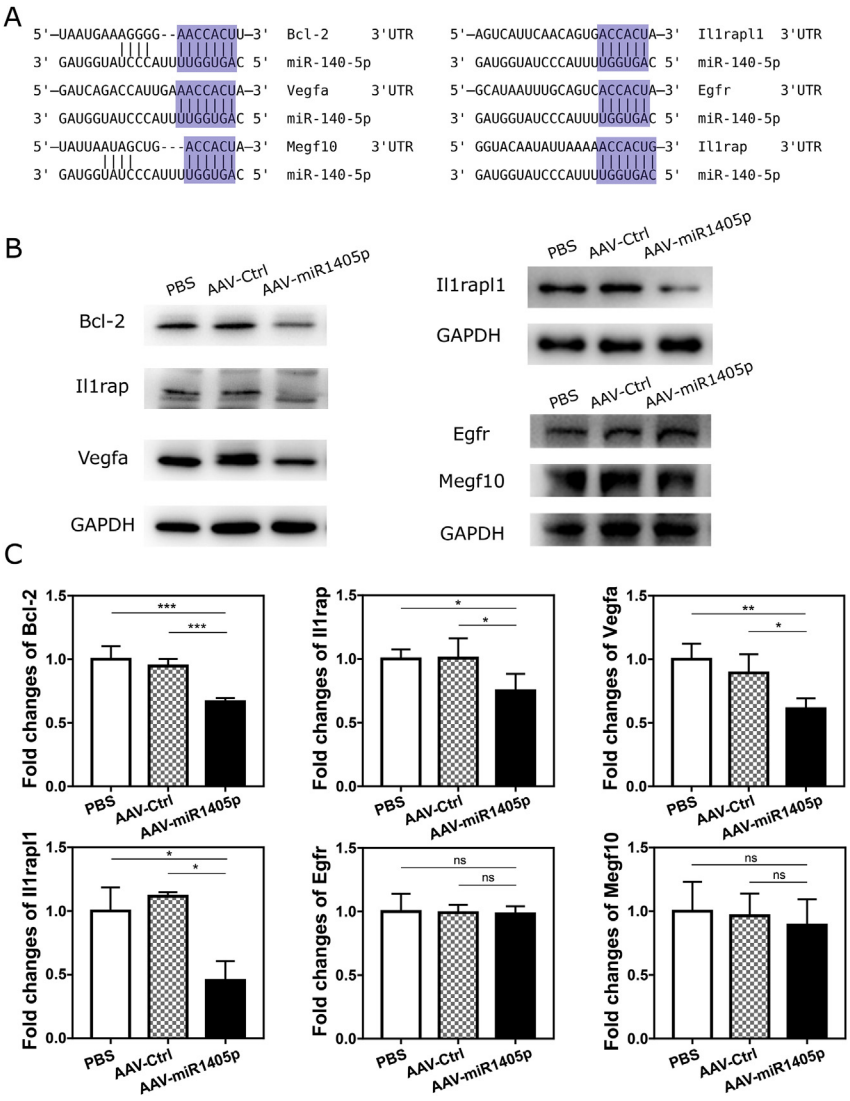

Fig. 6. Overexpression of miR-140-5p suppresses the expression of neuroplasticity and angiogenesis-related proteins in hippocampus tissue. **A**. The partial complementary sequences between miR-140-5p and the putative mRNA candidate targets. Purple shaded box represents the seed region of miR-140-5p. **B.** Western blotting analysis of Bcl-2, Vegfa, IL1rap, IL1rapl1, Megf10, and Egfr expression using protein samples isolated from hippocampus tissues of AAV-miR1405p, AAV-Ctrl, and PBS-treated mice. GAPDH was used as endogenous control for the proteins above. **C.** Quantification of hippocampal Bcl-2, Vegfa, IL1rap, IL1rapl1, Megf10, and Egfr from the Western blotting analysis. n = 4 or 5 per group. *P < 0.05; **P < 0.01; ***P < 0.001. (For interpretation of the references to color in this figure legend, the reader is referred to the Web version of this article.)

Recent studies have found that people who suffer from depression, especially recurrent depression, tend to have a significantly smaller hippocampus than non-suffering individuals (Schmaal et al., 2016). Sustained stress can cause the retraction of dendritic in hippocampal neurons, loss of pre-existing hippocampal neurons and decrease of neurogenesis in the adult hippocampus (Sapolsky, 2001). Antidepressants can protect the hippocampus by protecting hippocampal neurons from ischemic injury in a variety of ways. Treatment with antidepressants has been found to enhance neurogenesis in the dentate gyrus region. The phenomenon antidepressant effects are usually not seen until 2–4 weeks of continuous treatment suggests that it may be the time required for hippocampal neuron maturation and synaptic remodeling (Anacker et al., 2011). What's more, in our another a related research project, obvious up-regulation of miR-140-5p in the hippocampus region was detected in BCCAO mice (data wasn't shown here). Wherefore we have chosen the hippocampus region as our primary focus.

Our prior study found that the severity of neurological deficits is a significant risk factor for early-onset PSD, manifesting that acute ischemic stroke patients with higher NIHSS scores were more easily to suffer early-onset PSD (Zhang et al., 2016), and this funding was confirmed by other researchers (Meng et al., 2017; Karakus et al., 2017). So in the context of maximizing to imitate the cerebral ischemic status of the patients who are susceptible to late-onset PSD but avoid severity neurological impairment symptoms like serious hemiplegia, aphasia and sensory loss, a perfect animal model of stroke is necessary and pivotal. One of the most used rodent models for pathophysiology study of stroke is middle cerebral artery occlusion (MCAO), however, the drawbacks and pitfalls of the model must be appreciated that MCAO causes ischemic damage in the regions supplied by middle cerebral artery like cortex and striatum, resulting in inevitable neurological impairment with sensory-motor functioning. Transient bilateral common carotid artery occlusion in mice could induce obvious cerebral ischemic without obvious motor-sensory deficits, implying that it is more suitable for stimulating the status before late-onset PSD occurrence.

Brain-directed local injection of AAV vehicles is a straightforward way to gene transfer to the CNS. After the use of the AAV vector, widespread transduction in the brain was detected 2 weeks after injection (Miyake et al., 2015). Accordingly, we design a scheme that stereotactic injection was firstly conducted in C57BL/6 mice. 2 weeks later, transient bilateral common carotid artery occlusion surgeries were operated, under the above conditions, we explored whether some key target gene was actually altered by the overexpression of miR-140-5p in cerebral ischemia mice. C57BL/6 is the most susceptible strain to cerebral ischemia after occlusion of both common carotid arteries (CCAs). Bilateral CCAs occlusion for 20 min could cause severe ischemic in hippocampus and caudoputamen but an exception of cortex area in C57BL/6 mice, manifesting a selective ischemic neuronal death in the hippocampus region (Yang et al., 1997).

The neurogenic hypothesis suggests that the lack of neurogenesis (Jacobs et al., 2000) and synaptogenesis (Duman and Li, 2012)is one of the pathogenesis of depression (Peng and Bonaguidi, 2018). There existing varying degrees of data to support these interpretations. Selective serotonin reuptake inhibitors couldn't exert an antidepressant effect without neurogenesis, Evidence from preclinical studies shows that ventral hippocampal lesions or the inhibition and depletion of neurogenic can produce animal models of depression. These evidences collectively indicate that adult hippocampal neurogenesis serves as a key regulator for depression and can be used as a target for therapeutic drugs. In addition, recent studies have found that common factors regulate angiogenesis and neurogenesis in the human brain such as VEGF, BDNF, fibroblast growth factor-2 (FGF2) and insulin-like growth factor-1 (IGF1). Maura Boldrini et al. demonstrated that there was a casual relationship between angiogenesis and neurogenesis Reduced angiogenesis might affect neural progenitor cells (NPC) replication or survival in older MDD patients. The NPC number and capillary area correlated positively in the subgranular zone (SGZ) of the human brain (Boldrini et al., 2012). These interesting findings indicate that angiogenesis and adult hippocampal neurogenesis act as a beneficial contributor for the treatment and symptom amelioration of depression and the repair and regeneration process after stroke. Secondly, based on the above considerations, we have selected the following neurogenesis and angiogenesis-related targets for further in vivo verification.

Among the numerous predicted targets, we selected some hippocampal-specific, promising, or typical genes for subsequent exploration. The following is an introduction to the genes of interest. Interleukin-1 receptor accessory protein (IL1RAP) is a crucial component of receptor complexes in mediating immune responses to IL-1 family cytokines and organizes neuronal synaptogenesis and synapse formation in the brain (Yoshida et al., 2012). IL-1 receptor accessory protein-like 1 (IL1-RAPL1) also belongs to IL-1 receptor family and shares 52% homology with the IL1RAP, is highly expressed in brain areas such as the hippocampus, dentate gyrus, and entorhinal cortex (Ko et al., 2016). IL1-RAPL1 mediates excitatory synapse formation via trans-synaptic interaction with PTPδ (Yasumura et al., 2014). Multiple EGF-like domains 10 (Megf10) a class F scavenger receptor expressed on astrocytes in CNS, Tal Iram et al. demonstrated Megf10 was a receptor for C1q and involved in the synaptic pruning process in developing CNS and the clearance of synapses and apoptotic cells by astrocytes in the adult CNS (Iram et al., 2016). Epidermal growth factor receptor (EGFR) is a member of the HER superfamily of receptor tyrosine kinases, and binds to the ligands like EGF family of growth factors and transforming growth factor α to actuate many cellular processes including cell differentiation, metabolism, proliferation, and survival (Taylor et al., 2012). Furthermore, the apoptosis regulator Bcl-2 is a prototypical member of the Bcl-2 family and is uniquely positioned to crucially control neuronal cell survival through its regulation of both caspase-dependent and caspase-independent cell death pathways in the mature nervous system (Akhtar et al., 2004). Finally, Vegfa is not an unusual secreted mitogen associated with angiogenesis can notably enhance angiogenesis and decrease neurological deficits during stroke recovery.

To explore the biological effect of miR-140-5p on the hippocampus (in particular, DG region) and the potential downstream mediators of miR-140-5p, we performed AAV miR-overexpression vector injection in the hippocampal DG region of C57BL/6 mice. We demonstrated that up-regulated miR-140-5p could significantly inhibit the neurogenesis process and the capillary density of the DG region. The further Western blotting analysis confirmed that some neuroplasticity (IL1rap and IL1rapl1), angiogenesis (Vegfa) and apoptosis-related (Megf10) proteins expression were indeed significantly downregulated. Although we did not arrange experiments to detect the direct effect of miR-140-5p overexpression on the emotional changes in mice, at the micro level, we observed the important influence of miR-140-5p on neuroplasticity and capillary area, it may explain in part why it seems that the same stroke patients, some have gradually progressed into depression and some have not. Focusing attention on understanding the molecular substrates that the miR influences PSD and depression would be an important research avenue.

However, need to be interpreted in the context of limitations. First, the results of bioinformatics analyses should be experimentally validated. Second, the other two miRNAs (miR-221-3p and miR-1246) are also the significantly changed miRNAs and need to be further studied. A panel of several miRNAs maybe exhibits a better predictive effect for late-onset PSD. Thirdly, the lack of a group of depressed patients as a control, the absence of the assessment of cognitive impairment (like the MMSE and MoCA) and the long-term degree of disability (like the mRS) in stroke patients is also a flaw in the study design. Finally, we need to conduct a comprehensive validation with a detailed assessment in a large cohort containing multicenter clinical studies.

In summation, we found that there was a distinguishable miRNAs expression signature in PSD patients, enrichment analysis for the target genes indicated that neural plasticity mechanism may play an important role in the late-onset PSD developing. MiR-140-5p was significantly increased in the late-onset PSD patients' plasma. Acute ischemic stroke patients with a higher miR-140-5p on admission had more severe depressive symptoms three months after stroke. Overexpression of miR-140-5p has a significant suppression action on neurogenesis and capillary density of the DG region of cerebral ischemic mouse. These results have important implications in the search of biomarkers and predictors of late-onset PSD occurrence. These findings may also help us understand the molecular mechanisms of miR-140-5p in the development and progression of late-onset PSD, and furthermore provide new clues for the prevention, diagnostic and treatment of PSD.

Author contributions

L.Zeng and G-Y. Yang conceived and designed the study; H. Liang, Y. Zhang, J. He, X. Tu and K. Ding performed experiments; Y. Zhang contributed analytic tools; H. Liang analyzed the data; H. Liang, Y. Zhang and J. He wrote the paper.

Funding

This work has been supported by the National Natural Science Foundation of China (Grant 81471246 to L. Zeng, 81701059 to Lan Ye).

Conflicts of interest

The authors declare that they have no conflict of interest.

Acknowledgments

Not applicable.

Acknowledgements

This work was supported by the National Natural Science Foundation of China (Grant 81471246 to L. Zeng, 81701059 to Lan Ye). This research was supported with the resources and the use of facilities at the Neuroscience and Neuroengineering Center, Med-X Research Institute. The authors sincerely thank all the patients who participated in this study for making the research possible. All authors have approved the final version of this manuscript.

Appendix A. Supplementary data

Supplementary data to this article can be found online at https://doi.org/10.1016/j.jpsychires.2019.05.018.

Ethical approval

All procedures performed in studies involving human participants were in accordance with the ethical standards of the Medical Ethics Committee of the Ruijin Hospital, Shanghai Jiao Tong University School of Medicine and with the 1964 Helsinki declaration and its later amendments or comparable ethical standards.

All procedures performed in studies involving animals were in accordance with the ethical standards of Shanghai Jiao Tong University.

Informed consent

Informed consent was obtained from all individual participants included in the study.

Availability of data and material

The data (including the microarray data and deidentified participant data) that support the findings of this study are available from the corresponding author upon reasonable request.

References

Akhtar, R.S., Ness, J.M., Roth, K.A., 2004. Bcl-2 family regulation of neuronal development and neurodegeneration. Biochim. Biophys. Acta BBA - Mol. Cell Res., Bcl-2 family members: Integrat. Surviv. Death Signal. Physiol. Pathol. 1644, 189–203. https://doi.org/10/db2564.

Anacker, C., Zunszain, P.A., Cattaneo, A., Carvalho, L.A., Garabedian, M.J., Thuret, S., Price, J., Pariante, C.M., 2011. Antidepressants increase human hippocampal neurogenesis by activating the glucocorticoid receptor. Mol. Psychiatry 16, 738–750. https://doi.org/10/fsgm44.

Andersen, G., Vestergaard, K., Lauritzen, L., 1994. Effective treatment of poststroke depression with the selective serotonin reuptake inhibitor citalopram. Stroke 25, 1099–1104.

Berg, A., Palomäki, H., Lehtihalmes, M., Lönnqvist, J., Kaste, M., 2003. Poststroke depression: an 18-month follow-up. Stroke 34, 138–143.

Boldrini, M., Hen, R., Underwood, M.D., Rosoklija, G.B., Dwork, A.J., Mann, J.J., Arango, V., 2012. Hippocampal angiogenesis and progenitor cell proliferation are increased with antidepressant use in major depression. Biol. Psychiatry, Novel Pharmacotherapies Depress. 72, 562–571. https://doi.org/10/f38tms.

Bour, A., Rasquin, S., Aben, I., Boreas, A., Limburg, M., Verhey, F., 2010. A one-year follow-up study into the course of depression after stroke. J. Nutr. Health Aging 14, 488–493.

Bour, A., Rasquin, S., Limburg, M., Verhey, F., 2011. Depressive symptoms and executive functioning in stroke patients: a follow-up study. Int. J. Geriatr. Psychiatry 26, 679–686. https://doi.org/10/fd45qx.

Cao, D.-D., Li, L., Chan, W.-Y., 2016. MicroRNAs: key regulators in the central nervous system and their implication in neurological diseases. Int. J. Mol. Sci. 17. https://doi.org/10/f8s83f.

Catalanotto, C., Cogoni, C., Zardo, G., 2016. MicroRNA in control of gene expression: an overview of nuclear functions. Int. J. Mol. Sci. 17. https://doi.org/10/f9csf8.

Chang, K.-M., Harbron, C., South, M.C., n.d. An Exploration of Extensions to the RMA Algorithm vol. 10.

Duman, R.S., Li, N., 2012. A neurotrophic hypothesis of depression: role of synaptogenesis in the actions of NMDA receptor antagonists. Philos. Trans. R. Soc. Lond. B Biol. Sci. 367, 2475–2484. https://doi.org/10/f34svk.

Dweep, H., Sticht, C., Pandey, P., Gretz, N., 2011. miRWalk–database: prediction of possible miRNA binding sites by “walking” the genes of three genomes. J. Biomed. Inform. 44, 839–847. https://doi.org/10/d89f7r.

Goldberg, J.L., 2003. How does an axon grow? Genes Dev. 17, 941–958. https://doi.org/10/bqdmgf.

Hackett, M.L., Pickles, K., 2014. Part I: frequency of depression after stroke: an updated systematic review and meta-analysis of observational studies. Int. J. Stroke 9, 1017–1025. https://doi.org/10/f6pzpb.

Harrison, J.K., McArthur, K.S., Quinn, T.J., 2013. Assessment scales in stroke: clinimetric and clinical considerations. Clin. Interv. Aging 8, 201–211. https://doi.org/10/27m.

Ihaka, R., Gentleman, R., 1996. R: a language for data analysis and graphics. J. Comput. Graph. Stat. 5, 299–314. https://doi.org/10/gddc3n.

Iram, T., Ramirez-Ortiz, Z., Byrne, M.H., Coleman, U.A., Kingery, N.D., Means, T.K., Frenkel, D., Khoury, J.E., 2016. Megf10 is a receptor for C1Q that mediates clearance of apoptotic cells by astrocytes. J. Neurosci. 36, 5185–5192. https://doi.org/10/gfts2t.

Jacobs, B.L., van Praag, H., Gage, F.H., 2000. Adult brain neurogenesis and psychiatry: a novel theory of depression. Mol. Psychiatry 5, 262–269.

K Dar, S., Venigalla, H., Khan, A.M., Ahmed, R., Mekala, H.M., Zain, H., Shagufta, S., 2017. Post stroke depression frequently overlooked, undiagnosed, untreated. Neuropsychiatry 07. https://doi.org/10/gfdcx2.

Karakus, K., Kunt, R., Memis, C.O., Kunt, D.A., Dogan, B., Ozdemiroglu, F., Sevincok, L., 2017. The factors related to early-onset depression after first stroke. Psychogeriatrics 17, 414–422. https://doi.org/10/gfdcx5.

Kim, H.K., Tyryshkin, K., Elmi, N., Dharsee, M., Evans, K.R., Good, J., Javadi, M., McCormack, S., Vaccarino, A.L., Zhang, X., Andreazza, A.C., Feilotter, H., 2019. Plasma microRNA expression levels and their targeted pathways in patients with major depressive disorder who are responsive to duloxetine treatment. J. Psychiatr. Res. 110, 38–44. https://doi.org/10/gfx4hm.

Ko, J., Montani, C., Kim, E., Sala, C., 2016. Chapter 11 - mutations in synaptic adhesion molecules. In: Sala, C., Verpelli, C. (Eds.), Neuronal and Synaptic Dysfunction in Autism Spectrum Disorder and Intellectual Disability. Academic Press, San Diego, pp. 161–175. https://doi.org/10.1016/B978-0-12-800109-7.00011-X.

Krzywinski, M.I., Schein, J.E., Birol, I., Connors, J., Gascoyne, R., Horsman, D., Jones, S.J., Marra, M.A., 2009. Circos: an information aesthetic for comparative genomics. Genome Res. https://doi.org/10/dwmn6z.

Kuleshov, M.V., Jones, M.R., Rouillard, A.D., Fernandez, N.F., Duan, Q., Wang, Z., Koplev, S., Jenkins, S.L., Jagodnik, K.M., Lachmann, A., McDermott, M.G., Monteiro, C.D., Gundersen, G.W., Ma’ayan, A., 2016. Enrichr: a comprehensive gene set enrichment analysis web server 2016 update. Nucleic Acids Res. 44, W90–W97. https://doi.org/10/f8v4gw.

Larrea, E., Sole, C., Manterola, L., Goicoechea, I., Armesto, M., Arestin, M., Caffarel, M.M., Araujo, A.M., Araiz, M., Fernandez-Mercado, M., Lawrie, C.H., 2016. New concepts in cancer biomarkers: circulating miRNAs in liquid biopsies. Int. J. Mol. Sci. 17. https://doi.org/10/f8tntk.

Li, J., Zhao, Y.-D., Zeng, J.-W., Chen, X.-Y., Wang, R.-D., Cheng, S.-Y., 2014. Serum Brain-derived neurotrophic factor levels in post-stroke depression. J. Affect. Disord. 168, 373–379. https://doi.org/10/f6ggb6.

Lin, Q., Wei, W., Coelho, C.M., Li, X., Baker-Andresen, D., Dudley, K., Ratnu, V.S., Boskovic, Z., Kobor, M.S., Sun, Y.E., Bredy, T.W., 2011. The brain-specific microRNA miR-128b regulates the formation of fear-extinction memory. Nat. Neurosci. 14, 1115–1117. https://doi.org/10/fhppjh.

Lopez, J.P., Kos, A., Turecki, G., 2018. Major depression and its treatment: microRNAs as peripheral biomarkers of diagnosis and treatment response. Curr. Opin. Psychiatr. 31, 7–16. https://doi.org/10/gfx4jb.

López-Romero, P., 2011. Pre-processing and differential expression analysis of Agilent microRNA arrays using the AgiMicroRna Bioconductor library. BMC Genomics 12, 64. https://doi.org/10/bb66b7.

Ludwig, N., Leidinger, P., Becker, K., Backes, C., Fehlmann, T., Pallasch, C., Rheinheimer, S., Meder, B., Stähler, C., Meese, E., Keller, A., 2016. Distribution of miRNA expression across human tissues. Nucleic Acids Res. 44, 3865–3877. https://doi.org/10/f8ppbv.

Meng, G., Ma, X., Li, L., Tan, Y., Liu, Xiaohui, Liu, Xueyuan, Zhao, Y., 2017. Predictors of early-onset post-ischemic stroke depression: a cross-sectional study. BMC Neurol. 17. https://doi.org/10/gcmqc3.

Miyake, K., Miyake, N., Shimada, T., 2015. Gene delivery into the central nervous system (CNS) using AAV vectors. Gene Ther. - Princ. Chall. https://doi.org/10/gfttrp.

Narahari, A., Hussain, M., Sreeram, V., 2017. MicroRNAs as biomarkers for psychiatric conditions: a review of current research. Innov. Clin. Neurosci. 14, 53–55.

Peng, L., Bonaguidi, M.A., 2018. Function and dysfunction of adult hippocampal neurogenesis in regeneration and disease. Am. J. Pathol. 188, 23–28. https://doi.org/10/gft3rv.

Ritchie, M.E., Phipson, B., Wu, D., Hu, Y., Law, C.W., Shi, W., Smyth, G.K., 2015. Limma powers differential expression analyses for RNA-sequencing and microarray studies. Nucleic Acids Res. 43 e47–e47. https://doi.org/10/f7c4n5.

Robinson, R.G., Jorge, R.E., 2016. Post-stroke depression: a review. Am. J. Psychiatry 173, 221–231. https://doi.org/10/f8k37b.

Ruike, Y., Ichimura, A., Tsuchiya, S., Shimizu, K., Kunimoto, R., Okuno, Y., Tsujimoto, G., 2008. Global correlation analysis for micro-RNA and mRNA expression profiles in human cell lines. J. Hum. Genet. 53, 515–523. https://doi.org/10/bktxcc.

Santos, M., Kövari, E., Gold, G., Bozikas, V.P., Hof, P.R., Bouras, C., Giannakopoulos, P., 2009. The neuroanatomical model of post-stroke depression: towards a change of focus? J. Neurol. Sci., Vascular Dementia 283, 158–162. https://doi.org/10/b56wfp.

Sapolsky, R.M., 2001. Depression, antidepressants, and the shrinking hippocampus. Proc. Natl. Acad. Sci. U. S. A 98, 12320–12322. https://doi.org/10/bs7p32.

Schmaal, L., Veltman, D.J., van Erp, T.G.M., Sämann, P.G., Frodl, T., Jahanshad, N., Loehrer, E., Tiemeier, H., Hofman, A., Niessen, W.J., Vernooij, M.W., Ikram, M.A., Wittfeld, K., Grabe, H.J., Block, A., Hegenscheid, K., Völzke, H., Hoehn, D., Czisch, M., Lagopoulos, J., Hatton, S.N., Hickie, I.B., Goya-Maldonado, R., Krämer, B., Gruber, O., Couvy-Duchesne, B., Rentería, M.E., Strike, L.T., Mills, N.T., de Zubicaray, G.I., McMahon, K.L., Medland, S.E., Martin, N.G., Gillespie, N.A., Wright, M.J., Hall, G.B., MacQueen, G.M., Frey, E.M., Carballedo, A., van Velzen, L.S., van Tol, M.J., van der Wee, N.J., Veer, I.M., Walter, H., Schnell, K., Schramm, E., Normann, C., Schoepf, D., Konrad, C., Zurowski, B., Nickson, T., McIntosh, A.M., Papmeyer, M., Whalley, H.C., Sussmann, J.E., Godlewska, B.R., Cowen, P.J., Fischer, F.H., Rose, M., Penninx, B.W.J.H., Thompson, P.M., Hibar, D.P., 2016. Subcortical brain alterations in major depressive disorder: findings from the ENIGMA Major Depressive Disorder working group. Mol. Psychiatry 21, 806–812. https://doi.org/10/f8m2bg.

Shi, Y., Xiang, Y., Yang, Y., Zhang, N., Wang, S., Ungvari, G.S., Chiu, H.F.K., Tang, W.K., Wang, YiLong, Zhao, X., Wang, YongJun, Wang, C., 2015. Depression after minor stroke: prevalence and predictors. J. Psychosom. Res. 79, 143–147. https://doi.org/10/f3g538.

Sims, J.R., Gharai, L.R., Schaefer, P.W., Vangel, M., Rosenthal, E.S., Lev, M.H., Schwamm, L.H., 2009. ABC/2 for rapid clinical estimate of infarct, perfusion, and mismatch volumes. Neurology 72, 2104–2110. https://doi.org/10/djtpbx.

Snyder, J.S., Soumier, A., Brewer, M., Pickel, J., Cameron, H.A., 2011. Adult hippocampal neurogenesis buffers stress responses and depressive behaviour. Nature 476, 458–461. https://doi.org/10/dn3834.

Sturm, J.W., Donnan, G.A., Dewey, H.M., Macdonell, R.A.L., Gilligan, A.K., Srikanth, V., Thrift, A.G., 2004. Quality of life after stroke: the north east melbourne stroke incidence study (NEMESIS). Stroke 35, 2340–2345. https://doi.org/10/bgk2gf.

Sun, N., Li, Q.-J., Lv, D.-M., Man, J., Liu, X.-S., Sun, M.-L., 2014. A survey on 465 patients with post-stroke depression in China. Arch. Psychiatr. Nurs. 28, 368–371. https://doi.org/10/f6p65h.

Tavakolizadeh, J., Roshanaei, K., Salmaninejad, A., Yari, R., Nahand, J.S., Sarkarizi, H.K., Mousavi, S.M., Salarinia, R., Rahmati, M., Mousavi, S.F., Mokhtari, R., Mirzaei, H., 2018. MicroRNAs and exosomes in depression: potential diagnostic biomarkers. J. Cell. Biochem. 119, 3783–3797. https://doi.org/10/gdbstm.

Taylor, T.E., Furnari, F.B., Cavenee, W.K., 2012. Targeting EGFR for treatment of glioblastoma: molecular basis to overcome resistance. Curr. Cancer Drug Targets 12, 197–209.

Wang, J., Chen, J., Sen, S., 2016. MicroRNA as biomarkers and diagnostics. J. Cell. Physiol. 231, 25–30. https://doi.org/10/gfgpjs.

Wang, Y., Liu, M., Pu, C., 2017. 2014 Chinese guidelines for secondary prevention of ischemic stroke and transient ischemic attack: compiled by the Chinese Society of Neurology, Cerebrovascular Disease Group. Int. J. Stroke 12, 302–320. https://doi.org/10/f9xh5h.

Wongwandee, M., Tangwongchai, S., Phanthumchinda, K., 2012. Relationship between poststroke depression and ischemic lesion location. J. Med. Assoc. Thail. Chotmaihet Thangphaet 95, 330–336.

Yang, G., Kitagawa, K., Matsushita, K., Mabuchi, T., Yagita, Y., Yanagihara, T., Matsumoto, M., 1997. C57BL/6 strain is most susceptible to cerebral ischemia following bilateral common carotid occlusion among seven mouse strains: selective neuronal death in the murine transient forebrain ischemia. Brain Res. 752, 209–218. https://doi.org/10/drr4xv.

Yang, Y., Shi, Y.-Z., Zhang, N., Wang, S., Ungvari, G.S., Ng, C.H., Wang, Y.-L., Zhao, X.-Q., Wang, Y.-J., Wang, C.-X., Xiang, Y.-T., 2016. The disability rate of 5-year post-stroke and its correlation factors: a national survey in China. PLoS One 11, e0165341. https://doi.org/10/f9rd47.

Yasumura, M., Yoshida, T., Yamazaki, M., Abe, M., Natsume, R., Kanno, K., Uemura, T., Takao, K., Sakimura, K., Kikusui, T., Miyakawa, T., Mishina, M., 2014. IL1RAPL1 knockout mice show spine density decrease, learning deficiency, hyperactivity and reduced anxiety-like behaviours. Sci. Rep. 4. https://doi.org/10/gftszg.

Yoshida, T., Shiroshima, T., Lee, S.-J., Yasumura, M., Uemura, T., Chen, X., Iwakura, Y., Mishina, M., 2012. Interleukin-1 receptor accessory protein organizes neuronal synaptogenesis as a cell adhesion molecule. J. Neurosci. 32, 2588–2600. https://doi.org/10/f3wmp4.

Yu, G., 2018. clusterProfiler: an Universal Enrichment Tool for Functional and Comparative Study. https://doi.org/10/gffb9f.

Yu, G., Wang, L.-G., Han, Y., He, Q.-Y., 2012. clusterProfiler: an R Package for comparing biological themes among gene clusters. OMICS A J. Integr. Biol. 16, 284–287. https://doi.org/10/gdf33f.

Zhang, Y., Cheng, L., Chen, Y., Yang, G.-Y., Liu, J., Zeng, L., 2016. Clinical predictor and circulating microRNA profile expression in patients with early onset post-stroke depression. J. Affect. Disord. 193, 51–58. https://doi.org/10/f783t7.

Zhang, Y., He, J., Liang, H., Lu, W., Yang, G.-Y., Liu, J., Zeng, L., 2017. Diabetes mellitus is associated with late-onset post-stroke depression. J. Affect. Disord. 221, 222–226. https://doi.org/10/gfdb2z.

Zhao, F., Yue, Y., Li, L., Lang, S., Wang, M., Du, X., Deng, Y., Wu, A., Yuan, Y., Zhao, F., Yue, Y., Li, L., Lang, S., Wang, M., Du, X., Deng, Y., Wu, A., Yuan, Y., 2018. Clinical practice guidelines for post-stroke depression in China. Br. J. Psychiatry 40, 325–334. https://doi.org/10/gfdcx4.